

Preparation and characterization of inherently heat-sealable polyimides with high glass transition temperatures

Hongjiang Ni, Jingang Liu, Shiyong Yang

Laboratory of Advanced Polymer Materials, Institute of Chemistry, Chinese Academy of Sciences, Beijing 100190, China

Correspondence to: J. Liu (E-mail: liujg@iccas.ac.cn) and S. Yang (E-mail: shiyang@iccas.ac.cn)

ABSTRACT: A series of inherently heat-sealable copolyimides (CPIs) with high glass transition temperatures were synthesized from 2,3,3',4'-oxydiphthalic anhydride (aODPA) and bicomponent diamines, 4,4'-oxydianiline (ODA) and *para*-phenylenediamine (PDA). The PI chain rigidity was manipulated by the regulation of the diamine ratio, and its effects on the heat sealability and thermal resistance of the derived CPI films were investigated in detail. The results show that these films are in possession of both good heat sealability and thermal resistance due to the synergetic effect of the asymmetry of aODPA and the rigidity of PDA. It is also found that there exists one critical PDA content that distinguishes the heat-sealing behaviors of the CPI films, and the relevant mechanism was established. Especially for CPI-5, the heat-sealing strength is up to 350 N m⁻¹ simultaneously with a relatively high T_g of 310°C.

© 2015 Wiley Periodicals, Inc. J. Appl. Polym. Sci. 2016, 133, 43058.

KEYWORDS: asymmetry; glass transition temperature; heat-sealability; polyimide

Received 27 August 2015; accepted 16 October 2015

DOI: 10.1002/app.43058

INTRODUCTION

Excellent combined properties have made polyimides (PIs) good candidates for varieties of high-tech applications, such as electrical and electronic devices, advanced displays, energy and aerospace industries.^{1–5} Especially in the aerospace area, the requirement becomes more and more urgent for large-scale PI films that rely on the adhesive behaviors between PI films themselves. However, for common wholly aromatic PIs, existence of strong inter- and intramolecular interaction and lack of polar functional groups at the surfaces together with low surface free energy generally deteriorate the adhesive characteristics.⁶ To overcome this deficiency, much efforts have been performed including surface chemical treatment,^{7–9} surface plasma treatment,^{10,11} or surface coating with additional polymers (polytetrafluoroethylene, acrylic resin, etc.).^{12,13} But these methods tend to endow PIs with good adhesiveness at the expense of their intrinsic properties,¹⁴ such as the deterioration of mechanical strength due to surface damage, and the reduction of service temperature due to the inferior thermal resistant of coating materials.

On the other hand, as a facile method of bonding films, the heat-sealing technique is frequently utilized in polyolefin-packing industrial, only including thermal-pressing steps.¹⁵ Nevertheless, it is usually impossible to fabricate large-scale PI films with this technique due to the nonthermoplastic behavior of common PIs. Therefore, the development of inherently heat-sealable PIs is of much interest to the academia and industry. In view of the essence

of the heat-sealing of polymers, namely the interdiffusion and entanglement of molecular chains,¹⁶ the crucial issue of developing heat-sealing PIs is how to reinforce the thermoplasticity of PI films. Accordingly, one of the methodologies is to introduce flexible structures, such as ether, alkyl, and carbonyl linkages.^{17–19} However, the thermal properties of PIs tend to be compromised by the introduction of such groups.²⁰ For example, the T_g value of Kapton® KJ, a commercially available heat-sealable PIs containing large quantities of ether linkages, is only about 220°C.¹⁷

In order to mediate the conflict between the thermal resistance and heat sealability of PI films, some other methodologies have to be taken. Regarding the thermal resistance, the reinforcement of chain-rigidity would be of much benefit. As the simplest aromatic diamine, *para*-phenylenediamine (PDA) is an effective and convenient choice for the preparation of highly thermal-resistant PIs whose T_g values are usually higher than 300°C, such as 3,3',4,4'-biphenyl tetracarboxylic dianhydride (sBPDA)-PDA PI.²¹ However, these PDA-derived PIs generally exhibit no thermoplasticity because of their high chain-packing density, which also leads to the deteriorated solubility, even when PDA is coupled with the dianhydrides containing flexible linkages like 3,3',4,4'-oxydiphthalic anhydride (sODPA) and 3,3',4,4'-benzophenone-tetracarboxylic dianhydride (sBTDA).²² On the other hand, it is well known that asymmetrical dianhydrides are beneficial for the increasing of free-volume of PIs. This characteristic makes it possible to produce thermoplastic PIs.^{21,23} For

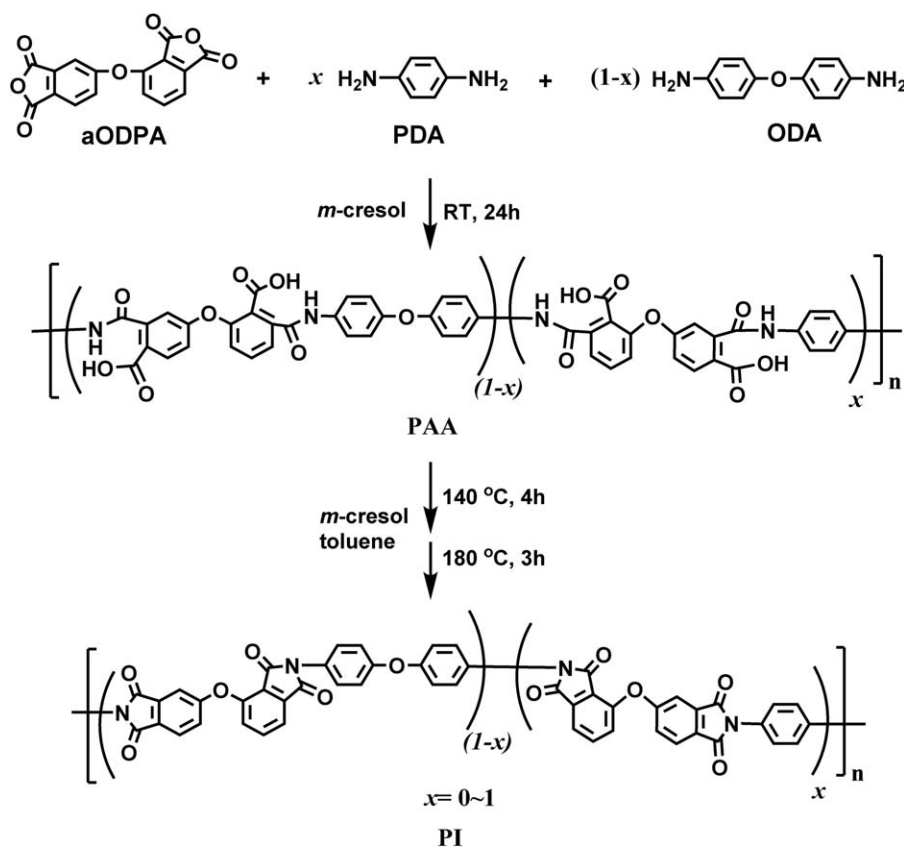


Figure 1. Synthesis of COPIs.

example, UBE Industries developed a heat-sealable PI film, Upilex[®] VT, whose thermoplastic layers consisted of the PI derived from an asymmetrical dianhydride, 2,3,3',4'-biphenyl tetracarboxylic dianhydride (aBPDA).²⁴ Recently, Yokota *et al.* reported a heat-sealable PI (ISAS-TPI) from another asymmetrical aromatic dianhydride, 2,3,3',4'-oxydiphthalic anhydride (aODPA), which has been successfully employed as membrane component for the solar sail.^{25,26}

Based on the aforementioned aspects, it is supposedly possible to develop heat-sealable PIs with high thermal resistance by the synergetic effect of PDA and aODPA. Unfortunately, to our knowledge, there is no detailed research regarding the heat-sealing or thermoplastic behaviors of aODPA-PDA-derived PI films. In this research, a series of copolyimides (CPIs) was synthesized from aODPA, PDA, and another diamine, 4,4'-oxydianiline (ODA) as the flexible component. The asymmetry of aODPA dianhydride and the flexibility of ODA diamine might endow the CPIs with good thermoplasticity while the rigidity of PDA might enhance the T_{gs} of the derived CPIs. Further, the CPI chain-rigidity might be easily manipulated by the regulation of diamine ratio, and therefore, its effects on the heat sealability and thermal resistance can be surveyed.

EXPERIMENTAL

Materials

2,3,3',4'-oxydiphthalic anhydride (aODPA), 4,4'-oxydianiline (ODA), and *para*-phenylenediamine (PDA) were purchased

from Tokyo Chemical Industry Co., Ltd. (TCI, Japan) and their chemical structures are shown in Figure 1. *N*-methyl-2-pyrrolidinone (NMP) was distilled prior to use and stored in 4 Å molecular sieves. The other commercially available reagents including *m*-cresol (Beijing Chemical Works, China) and isoquinoline (Alfa Aesar, USA) were used as received.

Characterization

Fourier-transform infrared (FTIR) spectra were measured with a Tensor 27 Fourier-transform spectrometer. H-nuclear magnetic resonances (¹H-NMR) spectra were performed on a Bruker Avance 400 spectrometer operating at 400 MHz in DMSO-*d*₆. X-ray photoelectron spectroscopy (XPS) data were obtained with an ESCALab220i-XL electron spectrometer from VG Scientific using a 300 W MgK α radiation. The cross-sectional morphology of the heat-sealing sample was observed by scanning electron microscope SEM (S-4800, HITACHI). The molecular weights were determined by size exclusion chromatography (SEC) on the system equipped with a Waters Pump, a differential refractive index detector (Optilab T-rEX, 25°C, 658 nm), and a laser light-scattering detector (DAWN RELIOS-II, 658 nm), of which eluent liquid was *N,N*-dimethylformamide (DMF) with 0.05 mol L⁻¹. The specific refractive index increment (dn/dc) was measured at the same conditions as those of SEC. Wide-angle X-ray diffraction (XRD) of the film was performed on a Rigaku D/max-2500 X-ray diffractometer (using Cu K α radiation at wavelength of 0.154 nm) over the range of 3–60°, at the scanning speed of 5°/min. The contact angle of the

Table I. PDA Contents of the Synthesized CPI in Diamines

| CPI | CPI-0 | CPI-1 | CPI-3 | CPI-5 | CPI-6 | CPI-7 | CPI-9 | CPI-10 |
|---------------------|-------|-------|-------|-------|-------|-------|-------|--------|
| PDA content (mol %) | 0 | 10 | 30 | 50 | 60 | 70 | 90 | 100 |

film was obtained on a DataPhysics-OCA 20 contact-angle measuring device.

Solubility was characterized as follows: 1.0 g of the PI resin was mixed into 9.0 g of the solvent tested (10 wt % solid content), which was stirred for 24 h at room temperature. The solubility was determined visually as three grades: completely soluble (++), partially soluble (+), and insoluble (-), wherein complete solubility indicates a homogenous and clean state without phase separation, precipitation, or gel formation, and insolubility indicates no change of the resin in the appearance.

Thermogravimetric analysis (TGA) was performed on a TA-Q50 thermal analysis system at a heating rate of 20°C min⁻¹ in nitrogen. Dynamic mechanical analysis (DMA) was recorded on a TA-Q800 thermal analysis system at a heating rate of 5°C min⁻¹ and a frequency of 1 Hz in nitrogen. Mechanical properties were determined by tensile testing at a drawing rate of 2.0 mm min⁻¹ according to GB 13022-91. Heat-sealing strengths were obtained by T-type peeling test in accordance with QB/T 2358-98. Both the above tests were performed on the Instron 3365 tensile apparatus and five specimens were needed for each PI film to give an average result.

Polymer Synthesis

As shown in Figure 1, the copolyimides (CPIs) were synthesized from aODPA and bicomponent diamines, PDA and ODA, with a molar ratio of PDA/ODA from 0/100 to 100/0 via a one-step high-temperature polycondensation procedure. The specific PDA contents of the eight synthesized CPIs are listed in Table I. As an example, the synthetic route of CPI-5 is illustrated as follows: in a 250 mL three-neck round flask equipped with a mechanical stirrer, a nitro inlet, a Dean-Stark trap, and a condenser, 3.2442 g (30 mmol) of PDA and 6.0072 g (30 mmol) of ODA and *m*-cresol were added. The mixture was stirred to a uniform state. Then 18.6126 g (60 mmol) of aODPA was added under the condition of ice-water bath, which produced a mixture of 16 wt % solid content. After the achievement of a homogeneous mixture, 49 g of toluene and a catalytic amount of isoquinoline were added at room temperature. The reaction mixture was heated to 140°C for dehydration and held for 4 h followed by another 3 h at 180°C after the elimination of water and toluene. When cooled, the viscous mixture was poured into ethanol slowly to precipitate for PI resin, which was dried for 24 h at 140°C.

PI films were prepared via the casting method as illustrated by the preparation of CPI-5 film: CPI-5 resin was dissolved in NMP for a homogeneous PI solution with a solid content of 15% which was filtered by a sand-core funnel to remove impurities. The solution was cast onto a glass-plate. Then the plate was thermally baked in accordance with the following temperature procedure: room temperature, 50°C/1 h, 80°C/1 h, 120°C/1 h, 160°C/1 h, 180°C/1 h, 240°C/2 h, 280°C/30 min, wherein

the heating rate was 2°C min⁻¹. After cooled down to room temperature, the glass plate was submerged into the deionized water to peel off the free-standing PI film. Finally, the film with the thickness of about 30 μm was obtained.

Fabrication of Heat-Sealing Samples

The heat sealing of CPI films was implemented with the hot-bar method on IDM L0001 Laboratory Heat Sealer, whose details were as follows (shown in Figure 2): a pair of film ribbons with the size of 90 × 70 mm² were overlapped and plugged into the platen molds for 20 mm width at a set temperature. The molds were kept for 1 min at 0.3–0.5 MPa. Then the once-hot-pressured sample was taken out and its two sides were reversed to repeat the process. To protect the films from the unexpected adhesion to the molds or each other caused by heat transfer, Kapton[®] film of 25 μm and 10 μm were covered outside and inserted into the two ribbons, respectively. After cooled down to room temperature, the heat-sealing sample was obtained and tailored for peeling test.

RESULTS AND DISCUSSION

Polymer Synthesis

The CPIs were easily prepared via one-step polymerization, due to their excellent solubility in *m*-cresol. The chemical structures of CPIs were characterized by the FT-IR spectra, XPS, and ¹H-NMR spectra. The FT-IR spectra of the monomers and the CPI films are shown in Figure 3 (for clarity, only three typical CPI curves were depicted). After imidization, the asymmetric and symmetric stretching vibration peaks of C=O around 1850 cm⁻¹ for aODPA and 1780 cm⁻¹ have disappeared as well as the signals of N–H between 3200 and 3400 cm⁻¹ for PDA and ODA. Instead, the asymmetric and symmetric stretching vibration peaks of C=O around 1780 and 1730 cm⁻¹ for imide group are observed, respectively. Besides, the stretching and deforming vibration peaks of imide C–N around 1380 and 740 cm⁻¹ as well as C–O–C around 1250 cm⁻¹ appear in the spectra. ¹H-NMR spectra of CPIs (CPI-0, 1, 3, and 5 as the representation, Figure 4) show that each signal is in good accordance with the structure of the molecular chain. In addition, the PDA contents based on feeding and NMR measurement are congruent. The successful conversion of anhydride group to imide group is further confirmed by the XPS. As shown by the XPS spectrum of O1s for CPI-0 (see the insert of Figure 4), the CPI peak can be only deconvoluted into two peaks: Peak 1 with the binding energy (BE) of 533.2 eV and Peak 2 of 531.7 eV which are attributed to the O1s of the diphenyl ether group and that of the imide carbonyl group, respectively, and the peak for the anhydride carbonyl group (~532.4 eV) are not found.²⁷ These results demonstrate that the CPIs with designed chemical structures have been successfully prepared.

The absolute molecular weights of the CPI resins were obtained by size exclusion chromatography (SEC), for which the specific

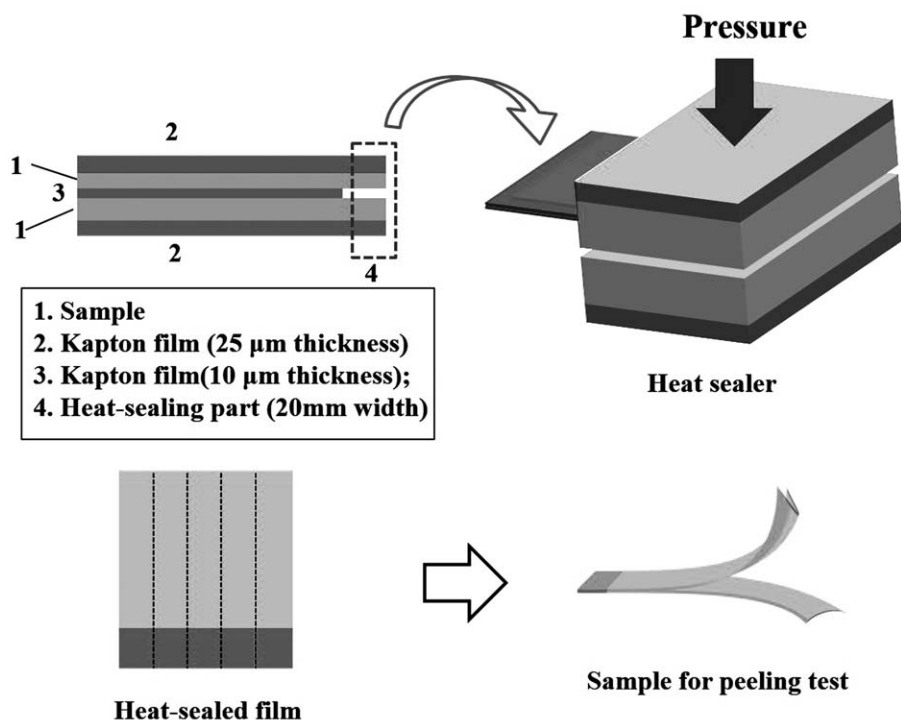


Figure 2. Schematic diagram of heat-sealing process.

refractive index increment (dn/dc) was first determined. According to the relationship between dn/dc and the refractive index of polymer, these CPIs should have approximate dn/dc values due to their similar chemical structures.^{27–30} Therefore, the dn/dc value of CPI-0 was measured and set as those of the other CPIs within an acceptable margin of error. To obtain the dn/dc of CPI-0, differential refractive indexes (DRIs) at four concentrations—0.25, 0.50, 0.75, and 0.10 g mL⁻¹—were measured. Then, the slope of the linear-fitting curve composed of these four points was calculated to give the dn/dc , that is, 0.2015 mL g⁻¹, as shown in Figure 5. The absolute molecular

weights of those CPIs were obtained thereof and are listed in Table II. The M_w s are around 10⁵ g mol⁻¹, as a premise of good mechanical properties for the corresponding films.

Solubility and Film Quality

Solution casting is an important method for the fabrication of PI film, for which solubility is a crucial factor. The rigid and

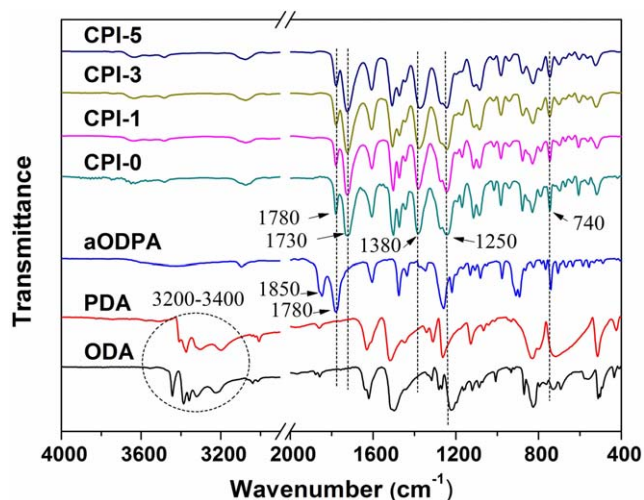


Figure 3. Typical FT-IR spectra for CPIs (CPI-0, 3, and 5). [Color figure can be viewed in the online issue, which is available at wileyonlinelibrary.com.]

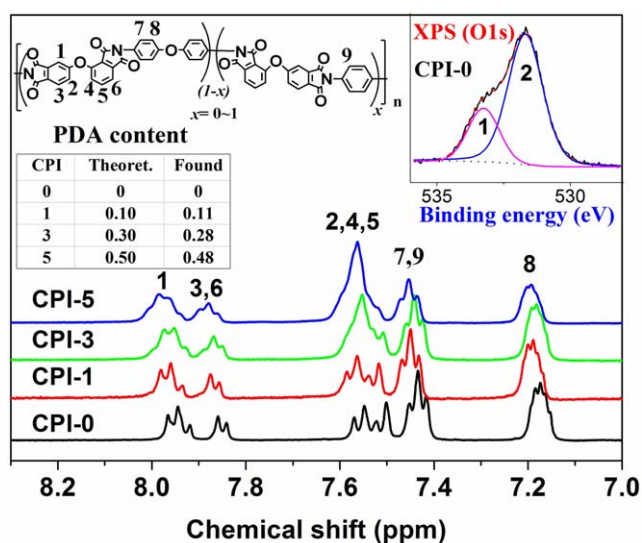


Figure 4. Typical ¹H-NMR spectra for CPIs (CPI-0, CPI-1, CPI-3, and CPI-5), and XPS spectrum of O1s for CPI-0 after deconvolution inserted at the upper-right corner (*Theoret.* and *Found* in the top-right table indicate PDA contents based on feeding and NMR measurement, respectively). [Color figure can be viewed in the online issue, which is available at wileyonlinelibrary.com.]

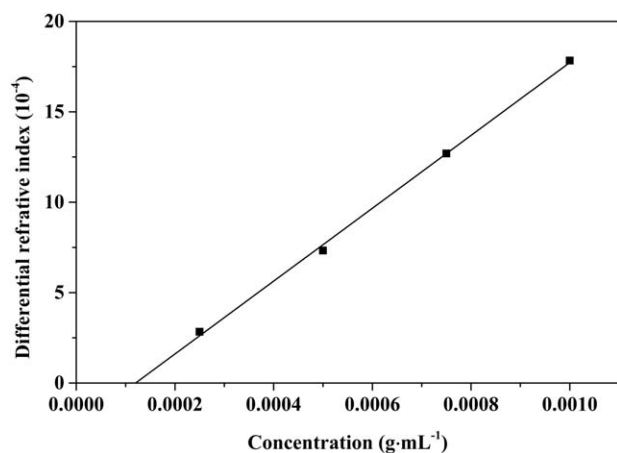


Figure 5. Differential refractive index as a function of concentration for CPI-0 (aODPA-ODA).

regular chemical structure renders PDA much difficult as the monomer for the preparation of soluble polyimide. Consequently, PDA-derived PI film is generally fabricated via two-step method including synthesis of polyamide acid (PAA) and subsequent heat imidization.³¹ Favorably, in our research, all these CPIs exhibit good solubility in the polar aprotic solvents, NMP, DMAc, DMF, and *m*-cresol, as shown in Table II. Besides, completely or partially soluble phenomena are even observed in the common solvents, CHCl₃ and CPA. The good solubility is attributed to the distorted and nonpolar structure of aODPA which decreases the interaction between the molecular chains. The weak chain interaction is also reflected in the XRD patterns of CPI films. As shown in Figure 6 (CPI-0, 5, and 10 as representatives), the CPIs exhibit broad diffractive peaks, indicating amorphous aggregating structures. The loose chain-packing density is of much benefit to the permeation of the solvent.

Benefitting from the good solubility of the CPI resins, the CPI films were facilely fabricated by the solution casting method. Then, the mechanical properties of the films were measured by tensile test. As shown in Table III, the tensile strengths (σ_t), tensile moduli (E), and elongations at break (ε) of films of

PI-1–PI-6 are around 100 MPa, 2.1 GPa, and 7%, respectively. The good mechanical properties benefit from the high molecular weights of the CPI resins.

Thermal Properties

Thermal properties of the PI films were estimated using TGA and DMA, and are listed in Table III. All the CPIs exhibit no obvious thermal decomposition before 500°C according to the TGA measurements (Figure 7). The temperatures at 5% weight loss ($T_{5\%}$) and 10% weight loss ($T_{10\%}$) are above 510 and 550°C, respectively. Furthermore, the residue weight ratios at 700°C approximate 60%. These results reflect the favorable thermal stability of the CPIs.

Due to the suppressed rotation of molecular chains,^{21,32,33} PIs derived from asymmetric dianhydrides tend to have better thermal resistance than those from the symmetric counterparts. Therefore, it would be of much advantage to choose aODPA as the anhydride in order to fabricate PIs with high T_g s. The DMA-tan δ curves of PIs are shown in Figure 8, and the T_g s obtained are listed in Table III. It is found that these CPIs have T_g s above 280°C, which indicates a high thermal-resistance. In addition, the thermal resistance has been further enhanced by the introduction of PDA, and the increased amplitude of T_g is higher than 60°C. The reinforcement of the chain rigidity caused by PDA should be responsible for this result.

Heat-Sealing Properties

Adequate interdiffusion of molecular chains between the film surfaces is the prerequisite for acquiring a good heat-sealing quality, which makes the thermoplasticity of PI films as a determinant factor. DMA is an effective method of characterizing the thermoplasticity of PI film, since the change of storage modulus (E') around T_g is affected by the chain mobility.³⁴ As shown in Figure 8, the E' s of the CPI films dropped rapidly and the dropped amplitudes are above 10^3 MPa °C⁻¹, indicating that they are in possession of good thermoplasticity^{26,35} and thus the heat-sealable potential. This favorable property should originate from the high free volume and weak chain interaction caused by the distorted structure of aODPA. However, it should be noticed that the storage moduli in rubber region (E'_r s) for CPI-

Table II. Absolute Molecular Weight and Solubility of the CPIs

| CPI | Absolute molecular weight ^a | | | Solubility ^b | | | | | | |
|--------|--|------------------------------|-----|-------------------------|------|-----|------------------|-------------------|-----|-----|
| | M_n (g mol ⁻¹) | M_w (g mol ⁻¹) | PDI | NMP | DMAc | DMF | <i>m</i> -cresol | CHCl ₃ | CPA | THF |
| CPI-0 | 75530 | 11290 | 1.5 | ++ | ++ | ++ | ++ | ++ | + | - |
| CPI-1 | 80530 | 15130 | 1.9 | ++ | ++ | ++ | ++ | ++ | + | - |
| CPI-3 | 55060 | 87070 | 1.6 | ++ | ++ | ++ | ++ | + | - | - |
| CPI-5 | 43760 | 77340 | 1.8 | ++ | ++ | ++ | ++ | - | - | - |
| CPI-6 | 106300 | 176000 | 1.7 | ++ | ++ | ++ | ++ | - | - | - |
| CPI-7 | 76030 | 11310 | 1.6 | ++ | ++ | ++ | ++ | - | - | - |
| CPI-9 | 70390 | 96870 | 1.4 | ++ | + | + | ++ | - | - | - |
| CPI-10 | Not soluble | | | ++ | - | - | ++ | - | - | - |

^aPDI: Polydispersity index, M_w/M_n .

^b++: completely soluble at room temperature; +: partially soluble; -: insoluble; NMP: *N*-methyl-2-pyrrolidinone; DMAc: *N,N*-dimethylacetamide; DMF: *N,N*-dimethylformamide; CPA: cyclopentanone; THF: tetrahydrofuran.

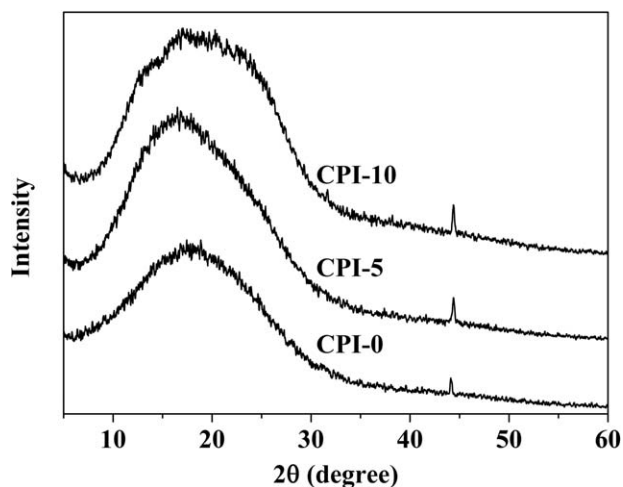


Figure 6. Typical wide-angle XRD patterns of CPI films (CPI-0, 5, and 10).

0–CPI-6 films are higher than those for CPI-7–CPI-10. According to the positive correlation between chain entanglement and E_r ,³⁶ the thermoplasticity of CPI-0–CPI-6 films should be superior to that of CPI-7–CPI-10, which is also suggested by the higher fluctuation intensity of E_r curves for the former films. Besides, the contact angles of these films were measured to characterize the surface wettability. Generally, high surface energy suggested by small contact angle is pursued to improve the adhesivity of PI film by varieties of means such as surface plasma treatment.¹¹ The contact angles of these CPI films are similar and below 70° , which is a favorable symptom for the heat sealability. As representatives, the contact angles of CPI-0, CPI-5, and CPI-10 films are shown in Figure 9.

Subsequently, the heat sealability of these CPI films was measured. The heat sealing of the PI films was carried out with the hot-bar method and the heat-sealing temperatures were set around the point $20\text{--}50^\circ\text{C}$ above the onset of DMA rubber region for each CPI film. The heat-sealing strengths are shown in Table IV and Figure 10. Generally, the peeling-failure modes

Table III. Thermal and Mechanical Properties of CPI Films

| CPI | Mechanical properties ^a | | | | Thermal properties ^b | | |
|-----|------------------------------------|-------|------------------|---------------|---------------------------------|---------------|-----------|
| | σ_t /MPa | E/GPa | ε /% | $T_{5\%}$ /°C | $T_{10\%}$ /°C | R_{w700} /% | T_g /°C |
| 0 | 110 | 2.4 | 8.9 | 537 | 554 | 61 | 285 |
| 1 | 97 | 2.1 | 7.4 | 549 | 565 | 61 | 295 |
| 3 | 99 | 2.1 | 7.1 | 548 | 571 | 63 | 299 |
| 5 | 102 | 2.5 | 6.7 | 549 | 572 | 62 | 310 |
| 6 | 103 | 2.4 | 7.3 | 544 | 567 | 62 | 314 |
| 7 | 115 | 2.9 | 6.7 | 530 | 564 | 64 | 321 |
| 9 | 115 | 2.8 | 7.3 | 511 | 553 | 62 | 330 |
| 10 | 117 | 2.4 | 7.5 | 526 | 552 | 60 | 350 |

^a σ_t : tensile strength; E: tensile modulus; ε : elongation at break.

^b T_g : glass transition temperature characterized by DMA; $T_{5\%}$, $T_{10\%}$: temperature at 5% and 10% weight loss, respectively; R_{w700} : residual weight ratio at 700°C in nitrogen.

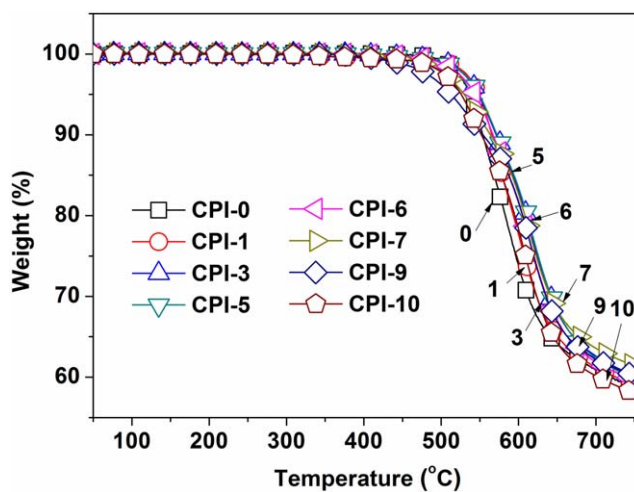


Figure 7. TGA curves of CPIs. [Color figure can be viewed in the online issue, which is available at wileyonlinelibrary.com.]

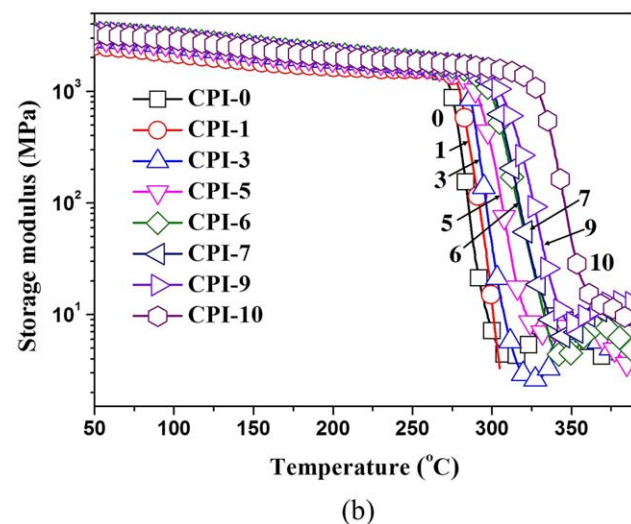
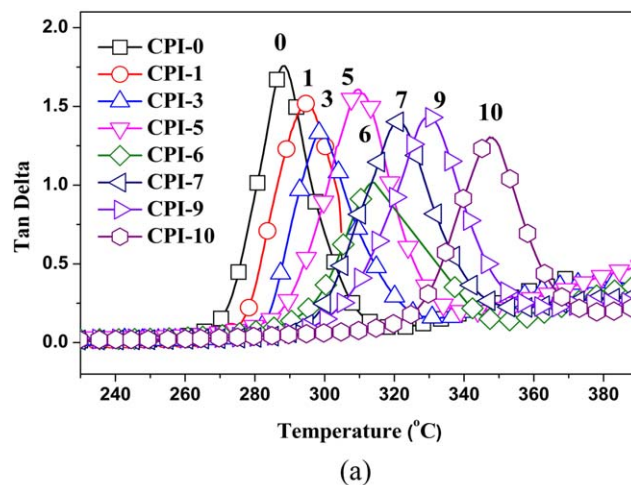


Figure 8. DMA curves of CPI films: (a) tan delta and (b) storage modulus. [Color figure can be viewed in the online issue, which is available at wileyonlinelibrary.com.]

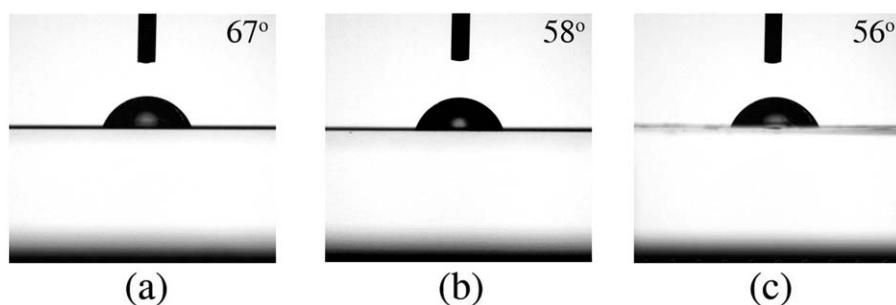


Figure 9. Typical contact angles of CPI films: (a) CPI-0, (b) CPI-5, and (c) CPI-10.

Table IV. Heat-Sealing Properties of the CPI Films

| CPI | 0 | 1 | 3 | 5 | 6 | 7 | 9 | 10 |
|--|-----|-----|-----|-----|-----|-----|-----|-----|
| Heat-sealing temperature/ $^{\circ}\text{C}$ | 340 | 350 | 360 | 370 | 380 | 390 | 400 | 400 |
| Heat-sealing strength/ N m^{-1} | 430 | 470 | 500 | 350 | 240 | 63 | 86 | 120 |
| Flexibility of heat-sealing parts ^a | Y | Y | Y | Y | Y | N | N | N |

^aY and N indicating the heat-sealing region has or does not have flexibility, respectively.

of heat-sealing sample can be divided into three types: peeling failure, edge-tearing failure, and combined failure.³⁷ Among these modes, tearing failure generally means effective heat sealing because the prerequisite for this mode is that the bonding strength of heat-sealing part is higher than the mechanical strength of the heat-sealing edge.

In the research, it is found that all the heat-sealing samples have failed in the edge-tearing mode. When the PDA contents equal or are lower than 60 mol %, the heat-sealing strengths are 240–500 N m^{-1} . Especially for PI-5, the value is up to 350 N m^{-1} simultaneously with a relatively high T_g of 308 $^{\circ}\text{C}$. However, as to the CPI films with PDA contents higher than 60 mol %, the heat-sealing strengths are much lower, namely only tens of newton per meter, although their failure also behaves as the edge-tearing mode. To discover the reasons, the heat-sealing parts for the CPI-7–CPI-10 films were examined and are found to be much brittle relative to the flexible bulks (fractured when folded), as shown by the right insert of Figure 10 (right, CPI-7 as the representative). Suggested by the deepening of the color to a large extent for the CPI films, the embrittlement phenomenon of the heat-sealing parts may be attributed to the chain degradation including the dehydrogenation of aromatic ring, splitting of aromatic ether, and hydroxylation of aromatic ring, as indicated by the sODPA-ODA PI at high temperatures (around 400 $^{\circ}\text{C}$).³⁸ However, the surface of the CPI film seems still apparently intact when imidized at the high temperature, as demonstrated by its SEM surface micrograph (see the left insert of Figure 10).

In order to find the distinction between the heat sealability of CPI films with relatively low and high PDA contents at a smaller scale, the cross-sectional morphologies of the heat-sealing parts of CPI films were examined. It is found that heat-sealing interfaces have disappeared for CPI films with PDA contents below 60 mol %, but are rather obvious for those with

PDA contents up the critical point. As the typical examples, the cross-sectional micrographs of heat-sealing parts for CPI-5 and CPI-7 films are shown in Figure 11 since these two films have the weakest and strongest thermoplasticity among CPI films with PDA contents below and above 60 mol %, respectively. The distinction between them suggests that the diffusion of molecular chains for CPI films with PDA contents above 60% is not as deep as that below 60%. Therefore, regardless of the tearing-failure mode, the heat-sealing of CPI-7–CPI-10 films may be not effective. This inefficiency should stem from the non-negligible detriment of excessive PDA to the chain mobility, which might be implied by the DMA-storage modulus curves as illustrated before (Figure 8).

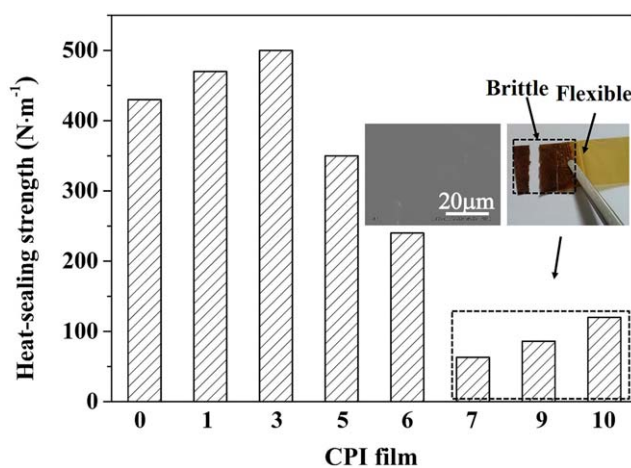


Figure 10. Histogram of heat-sealing strengths of CPI films: SEM surface micrograph of the film imidized at 380 $^{\circ}\text{C}$ (left) and apparent morphology of the heat-sealing sample after folding (right) for CPI-7 were inserted at the upper-right corner. [Color figure can be viewed in the online issue, which is available at wileyonlinelibrary.com.]

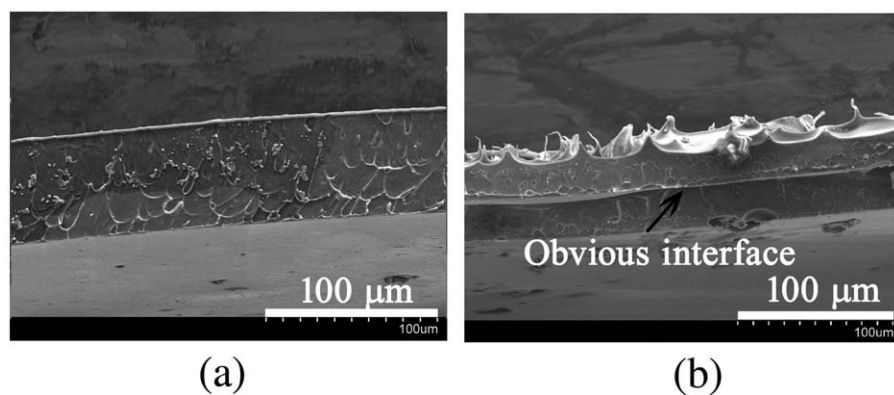


Figure 11. Typical SEM cross-sectional micrographs of heat-sealing parts for CPI films: (a) CPI-5 and (b) CPI-7.

CONCLUSIONS

Inherently heat-sealable copolyimides (CPIs) with elevated glass transition temperatures (T_g) were successfully synthesized from an asymmetrical aromatic dianhydride, 2,3,3',4'-oxydiphthalic anhydride (aODPA), 4,4'-oxydianiline (ODA), and *para*-phenylenediamine (PDA) via one-step high-temperature method. Effects of the PI chain rigidity on properties including T_g and heat-sealability have been surveyed by regulating the ratios of the rigid moiety (PDA) to the flexible one (ODA). It is found that benefitting from the synergetic effect of aODPA and PDA, these films exhibit both good heat sealability and improved thermal resistance. Relative to the completely ODA-derived PI system, the increment of T_g could be up to 65°C. The PDA content of 60 mol % is confirmed as the critical point diverging the heat sealability of the CPI films into two distinct regions, below which the heat sealability is superior. This phenomenon may be attributed to the disadvantageous effect of PDA on the PI thermosplasticity. Especially for CPI-5, the heat-sealing strength is up to 350 N m⁻¹ simultaneously with a relatively high T_g of 310°C. The current work might be beneficial for improving the service temperatures of PI films especially when used as the large-scale configuration in high-tech areas.

ACKNOWLEDGMENTS

Financial support from the Basic Research Program of China (973 Program) (2014CB643605) and National Natural Science Foundation of China (51173188) is gratefully acknowledged.

REFERENCES

- Liaw, D. J.; Wang, K. L.; Huang, Y. C.; Lee, K. R.; Lai, J. Y.; Ha, C. S. *Prog. Polym. Sci.* **2012**, *37*, 907.
- Coletta, E.; Toney, M. F.; Frank, C. W. *J. Appl. Polym. Sci.* **2015**, *132*.
- Liu, J.; Nakamura, Y.; Ogura, T.; Shibasaki, Y.; Ando, S.; Ueda, M. *Chem. Mater.* **2008**, *20*, 273.
- Tseng, C. Y.; Ye, Y. S.; Cheng, M. Y.; Kao, K. Y.; Shen, W. C.; Rick, J.; Chen, J. C.; Hwang, B. J. *Adv. Energy Mater.* **2011**, *1*, 1220.
- Pater, R. H.; Curto, P. A. *Acta Astronaut.* **2007**, *61*, 1121.
- Awaja, F.; Gilbert, M.; Kelly, G.; Fox, B.; Pigram, P. J. *Prog. Polym. Sci.* **2009**, *34*, 948.
- Park, S. J.; Lee, E. J.; Kwon, S. H. *Bull. Korean Chem. Soc.* **2007**, *28*, 188.
- Saenger, K. L.; Tong, H. M.; Haynes, R. D. *J. Polym. Sci. Part C: Polym. Lett.* **1989**, *27*, 235.
- Kim, H. J.; Park, Y. J.; Choi, J. H.; Han, H. S.; Hong, Y. T. *J. Ind. Eng. Chem.* **2009**, *15*, 23.
- Lin, Y. S.; Liu, H. M.; Chen, H. T. *J. Appl. Polym. Sci.* **2006**, *99*, 744.
- Lin, Y. S.; Liu, H. M.; Chen, C. L. *Surf. Coat. Technol.* **2006**, *200*, 3775.
- LaCOURT, P. WO Pat. WO1993014933 **1993**,
- Kundinger, E. F.; Klimesch, E.; Zengel, H. G.; Lasher, J. D. *US Pat. US4705720* **1987**,
- Jeun, J. P.; Shin, J. W.; Nho, Y. C.; Kang, P. H. *J. Ind. Eng. Chem.* **2009**, *15*, 56.
- Tetsuya, T.; Hashimoto, Y.; Ishiaku, U. S.; Mizoguchi, M.; Leong, Y. W.; Hamada, H. *J. Appl. Polym. Sci.* **2006**, *99*, 513.
- Stehling, F. C.; Meka, P. *J. Appl. Polym. Sci.* **1994**, *51*, 105.
- Kreuz, J. A.; Kanakarajan, K. US Pat. US5298331-a **1994**,
- Krause, E.; Yang, G. M.; Sessler, G. M. *Polym. Int.* **1998**, *46*, 59.
- Ratta, V.; Ayambem, A.; McGrath, J. E.; Wilkes, G. L. *Polymer* **2001**, *42*, 6173.
- Ni, H.; Liu, J.; Wang, Z.; Yang, S. *J. Ind. Eng. Chem.* **2015**, *28*, 16.
- Hasegawa, M.; Sensui, N.; Shindo, Y.; Yokota, R. *J. Polym. Sci. Part B: Polym. Phys.* **1999**, *37*, 2499.
- Ree, M.; Kim, K.; Woo, S. H.; Chang, H. *J. Appl. Phys.* **1997**, *81*, 698.
- Sasaki, T.; Moriuchi, H.; Yano, S.; Yokota, R. *Polymer* **2005**, *46*, 6968.
- Yamaguchi, H. *J. Photopolym. Sci. Technol.* **2003**, *16*, 233.
- Tsuda, Y.; Mori, O.; Funase, R.; Sawada, H.; Yamamoto, T.; Saiki, T.; Endo, T.; Yonekura, K.; Hoshino, H.; Kawaguchi, J. *Acta Astronaut.* **2013**, *82*, 183.
- Yokota, R.; Miyauchi, M. *Astrophys. Space. Sci. Proc.* **2013**, *32*, 303.

27. Ektessabi, A. M.; Hakamata, S. *Thin Solid Films* **2000**, 377–378, 621.
28. Yang, C. J.; Jenekhe, S. A. *Chem. Mater.* **1995**, 7, 1276.
29. Ioan, S.; Filimon, A.; Avram, E. *J. Macromol. Sci. Part B: Phys.* **2005**, B44, 129.
30. Groh, W.; Zimmermann, A. *Macromolecules* **1991**, 24, 6660.
31. Takizawa, K.; Wakita, J.; Azami, S.; Ando, S. *Macromolecules* **2011**, 44, 349.
32. Hasegawa, M.; Sensui, N.; Shindo, Y.; Yokota, R. *Macromolecules* **1999**, 32, 387.
33. Ding, M. *Prog. Polym. Sci.* **2007**, 32, 623.
34. Ree, M.; Park, Y. H.; Shin, T. J.; Nunes, T. L.; Volksen, W. *Polymer* **2000**, 41, 2105.
35. Yu, X.; Zhao, X.; Liu, C.; Rai, Z.; Wang, D.; Dang, G.; Zhou, H.; Chen, C. *J. Polym. Sci. Part A: Polym. Chem.* **2010**, 48, 2878.
36. Ferry J. D. 3rd ed. *Viscoelastic Properties of Polymer*, Wiley: New York, **1980**.
37. Meka, P.; Stehling, F. C. *J. Appl. Polym. Sci.* **1994**, 51, 89.
38. Saeed, M. B.; Zhan, M. *Eur. Polym. J.* **2006**, 42, 1844.